Available online at www.sciencedirect.com
SCIENCE DIRECT®
Journal of Molecular Catalysis A: Chemical 231 (2005) 247–254
JOURNAL OF MOLECULAR CATALYSIS A: CHEMICAL
www.elsevier.com/locate/molcata

Preparation, characterization, and catalytic activity of NiMg catalysts supported on mesoporous alumina for hydrodechlorination of *o*-dichlorobenzene

Pil Kim, Younghun Kim, Heesoo Kim, In Kyu Song, Jongheop Yi *

School of Chemical Engineering, Institute of Chemical Processes, Seoul National University, Shinlim-dong, Kwanak-ku, Seoul 151-742, Republic of Korea

Received 13 November 2004; accepted 8 January 2005

Abstract

Chemical templates containing binary metal components were prepared by controlling pH of a mixed solution of magnesium stearate and nickel salt. The resulting templates were used as structure-directing agents and bimetallic sources in the preparation of porous NiMg-Al_2O_3 catalysts, where $Al(OBu)_3$ was used as an aluminum source. Both NiMg-NP (a NiMg-Al_2O_3 catalyst templated by a NH_4OH-treated precipitate) and NiMg-HS (a NiMg-Al_2O_3 catalyst templated by a HCl-treated solution) catalysts showed almost the same physical properties. However, chemical properties of these catalysts such as metal reducibility and metal-support interaction were different depending on the identity of templates. Compared to the NiMg-NP catalyst, the NiMg-HS catalyst exhibited weak interaction between metal and support, resulting in more intensive metal aggregation. For comparison purpose, Ni and NiMg catalysts supported on mesoporous alumina were also prepared by a conventional impregnation method. In the hydrodechlorination of *o*-dichlorobenzene, the secondary metal component (magnesium) enhanced the catalytic activity and inhibited the catalyst deactivation. Among the catalysts employed in this work, the NiMg-NP catalyst, which retained a homogeneously mixed metallic state, was the most active in the catalytic reaction and was the most resistant against deactivation.

Keywords: Chemical template; Mesoporous alumina; Bimetallic supported catalyst; Hydrodechlorination of *o*-dichlorobenzene; Nickel and magnesium

1. Introduction

Mesoporous materials prepared by a self-assembled surfactant aggregate have been widely studied and employed in many fields of material science and engineering due to their remarkable features such as high surface area, large pore volume, and narrow pore size distribution [1–14]. These materials are potentially important as highly efficient catalyst supports due to the merit of controllable porosity that makes supported catalysts have desirable level of diffusion efficiency. Among mesoporous materials, mesoporous alumina has attracted much attention as a catalyst support in the petrochemical industry. Ionic or neutral surfactants have been widely used as chemical templates in the preparation of mesoporous alumina by templating methods [5–7,15,16]. It is well known that mesoporous aluminas have a three-dimensional interconnected pore system in the form of sponge-like structure, which is a great advantage in the catalytic applications [17–23].

Mesoporous aluminas having high surface area with uniform pore size distribution have been investigated for use as catalyst supports in the hydrodechlorination reactions [17,18]. In the early stage of our researches, these aluminas were found to be efficient supports for the preparation of finely dispersed Ni-Al_2O_3 catalysts, until some problems have been noted [17,18]. One problem was pore blocking by metal species after the thermal treatment, which eventually acted as a barrier against the diffusion of reaction species. The other problem was aluminum dissolution occurred in the im-

* Corresponding author. Tel.: +82 2 880 7438; fax: +82 2 888 7295.
E-mail address: jyi@snu.ac.kr (J. Yi).

1381-1169/$ – see front matter © 2005 Elsevier B.V. All rights reserved.
doi:10.1016/j.molcata.2005.01.018

pregnation step of metal precursor, resulting in the formation of less active nickel aluminate spinel in the hydrotreating reactions. In order to overcome these problems, we developed a new method for the synthesis of mesoporous Ni-Al_2O_3 catalyst [11]. It was revealed that magnesium ion of the magnesium stearate could be substituted with nickel ion of nickel nitrate by the treatment with HCl or NH_4OH to yield nickel stearate. The resulting nickel stearate was successfully used for the preparation of highly dispersed mesoporous Ni-Al_2O_3 catalyst. Although this method using nickel stearate can be a simple route for the preparation of mesoporous Ni-Al_2O_3 catalyst, the resulting catalyst contains only a single metal component. For more versatile application, it is desirable to prepare bimetallic catalysts with mesoporosity. It is known that bimetallic catalysts, compared to mono-metal catalysts, have several beneficial effects in terms of catalyst deactivation, product selectivity, and catalytic performance, owing to the electronic or geometric effect of metal surfaces referred to as an alloying effect [24–28].

In this work, bimetallic NiMg-stearates were prepared by controlling pH of the mixed solutions of magnesium stearate and nickel nitrate, and these surfactants were then used as structure directing agents and bimetallic sources for the synthesis of mesoporous NiMg-Al_2O_3 catalysts. The supported bimetallic catalysts were applied to the model hydrodechlorination reaction of *o*-dichlorobenzene (a toxic chemical in an environmental point of view).

2. Experimental

2.1. Synthesis of bimetallic NiMg-stearate from magnesium stearate

Mole ratio of magnesium stearate with respect to HCl or NH_4OH was precisely controlled to be 1:2.5. Appropriate amounts of magnesium stearate and nickel nitrate were dissolved in *sec*-butyl alcohol, and the pH of the mixed solution was then adjusted with HCl or NH_4OH. Due to the formation of different metal salts, the color of the mixed solution was changed from lime-green into dark-green after the addition of HCl, and from lime-green into lime-blue after the addition of NH_4OH. This mixture was stirred for 1 h, and the resulting product was then separated by centrifugation. The solution from the HCl-treated reactant and the solid precipitate from the NH_4OH-treated reactant were separately used as a structure directing agent and bimetallic source.

2.2. Preparation of NiMg-Al_2O_3

Bimetallic NiMg-stearate and aluminum *sec*-butoxide were used as a chemical template and an aluminum precursor, respectively. The aluminum source and chemical template were separately dissolved in *sec*-butyl alcohol, and the two solutions were then mixed. Small amounts of water were slowly added to the mixture at a rate of 1 ml/min. The resulting suspension was further stirred for 24 h, and then it was dried at 80 °C for 48 h. Solid product was finally calcined for 6 h at 500 °C in air. The NiMg-Al_2O_3 catalysts prepared using HCl-treated solution and NH_4OH-treated precipitate were denoted as NiMg-HS and NiMg-NP, respectively. The NiMg-Al_2O_3 catalysts were also prepared using NH_4OH-treated solution and HCl-treated precipitate. However, these catalysts showed low metal concentration, poor mesoporosity, and low catalytic performance. Therefore, our investigation was mainly focused on the NiMg-Al_2O_3 catalysts prepared using HCl-treated solution and NH_4OH-treated precipitate, i.e., NiMg-NP and NiMg-HS catalysts.

2.3. Preparation of Ni and NiMg catalysts impregnated on mesoporous alumina (MA)

For comparison and reference, Ni and NiMg catalysts impregnated on mesoporous alumina were prepared. At first, mesoporous alumina (denoted as MA) was prepared by a post-hydrolysis method [3] for use as a support. A typical synthesis procedure of the mesoporous alumina is as follows. Appropriate amounts of Al(*sec*-BuO)$_3$ and stearic acid were separately dissolved in *sec*-butyl alcohol, and the two solutions were then mixed. Water was added to the mixture at a rate of 1 ml/min, until a white precipitate was formed. The resulting slurry was further stirred for 24 h, and subsequently, it was dried in air. The crude product was calcined at 500 °C for 6 h with a stream of air. Ni/MA and NiMg/MA catalysts were prepared by a conventional impregnation method. The loadings of each metal component were adjusted to be ca. 10 and 5 wt.% for Ni and Mg, respectively.

2.4. Characterization

X-ray diffraction (XRD, M18XHF-SRA, MAC/Science) measurements were carried out in order to investigate phase transformation and particle size of the catalysts. Adsorption isotherms of nitrogen were obtained with an ASAP-2010 (Micromeritics) apparatus. Pore size distribution was determined by the BJH method applied to the desorption branch of the nitrogen isotherm. The Ni particles on the catalyst surfaces were imaged by transmission electron microscopy (TEM, Joel, JXA-8900R) using an ultrasonically dispersed catalyst sample (in ethanol) deposited on a carbon grid. Temperature-programmed reduction (TPR) measurements were carried out in a conventional flow system with a moisture trap connected to a TCD at temperatures ranging from room temperature to 900 °C with a heating rate of 10 °C/min. For the TPR measurements, a mixed stream of H_2 (2 ml/min) and N_2 (20 ml/min) was used for 0.1 g of the catalyst sample. Temperature-programmed desorption (TPD) profiles of hydrogen were obtained in a conventional flow system equipped with a TCD. Prior to the TPD experiments, the catalysts were reduced with a stream of H_2 at 450 °C for 3 h. Physically adsorbed hydrogen was removed

Table 1
Surface area, pore volume, and metal loading of the supported catalysts

	NP	HS	MA	Ni/MA[a]	NiMg/MA[a]
Surface area[b] (m^2/g)	318	234	376	234	161
Pore volume[c] (cm^3/g)	0.45	0.32	0.76	0.32	0.28
Metal loading[d] (wt.%)					
Ni	7.25	8.17	–	10.3	10.4
Mg	4.01	4.05	–	–	4.9

[a] Catalysts impregnated on mesoporous alumina.
[b] Calculated by the BET equation.
[c] BJH adsorption pore volume.
[d] Measured by ICP–AES.

by evacuation at a pressure of 2×10^{-2} Torr. The temperature was raised up to 800 °C with a ramping rate of 5 °C/min using Ar (10 ml/min) as a carrier gas for 0.5 g of catalyst sample.

2.5. Hydrodechlorination of o-dichlorobenzene

Hydrodechlorination of *o*-dichlorobenzene was carried out in a continuous flow fixed-bed reactor at an atmospheric pressure. Each catalyst (0.2 g) with a size of 150–200 μm was charged into a tubular quartz reactor, and activated with a mixed stream of H_2 (20 ml/min) and N_2 (20 ml/min) at 450 °C for 3 h. The reaction temperature was maintained at 300 °C. The reactant, *o*-dichlorobenzene, was vaporized by passing a pre-heating zone and fed into the reactor continuously at a rate of 5.00×10^{-3} mol/h. The products were periodically sampled and analyzed with GC–MS and GC (HP 5890 II, FID). Catalytic reactions were carried out several times for each catalyst under the same conditions. In each run, the conversion of *o*-dichlorobenzene was oscillated within an error range of ±2%.

3. Results and discussion

3.1. Metal loadings and textural properties

In a previous work [11], it was reported that nickel stearate could be prepared from a mixed solution of magnesium stearate and nickel nitrate by adjusting pH of the solution. In this study, therefore, pH of the mixed solution was precisely controlled in order to obtain a chemical template containing two metal components, nickel and magnesium, in a single template. As summarized in Table 1, ICP–AES analyses revealed that all the catalysts derived from these chemical templates retained bimetallic systems. This result also shows that magnesium ions in the magnesium stearate were partially replaced by nickel ions.

Nitrogen adsorption–desorption isotherms and pore size distributions of NiMg-Al_2O_3 catalysts are shown in Fig. 1. Textural properties are also listed in Table 1. The NiMg-NP and NiMg-HS catalysts showed narrow pore size distributions with well-developed framework mesoporosity, and their hysteresis loops appeared within a relative pressure ranging

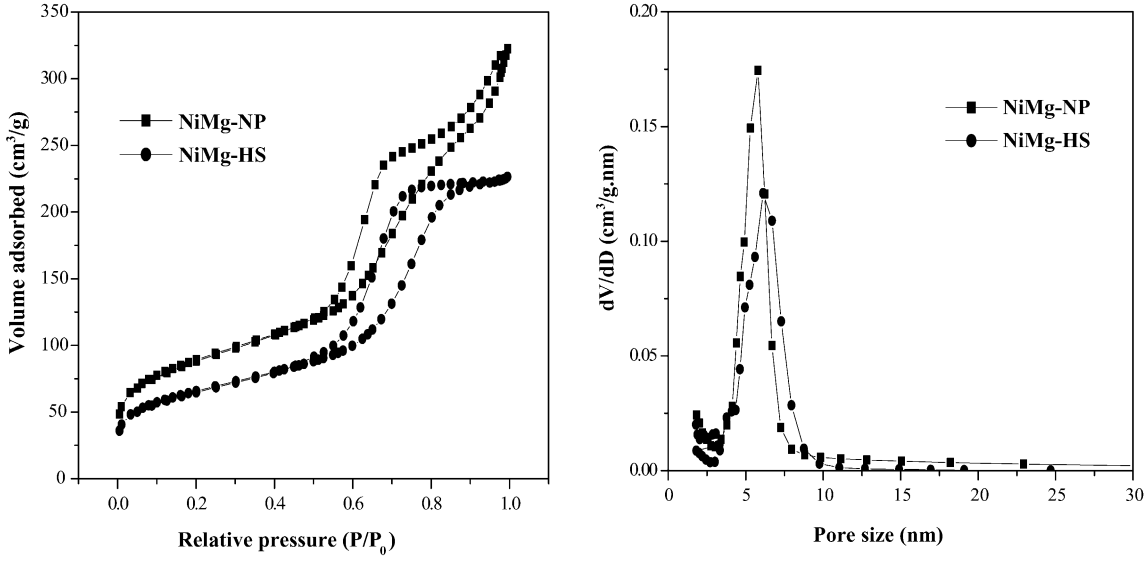

Fig. 1. (a) N_2 adsorption–desorption isotherms, and (b) pore size distributions of NiMg-Al_2O_3 catalysts.

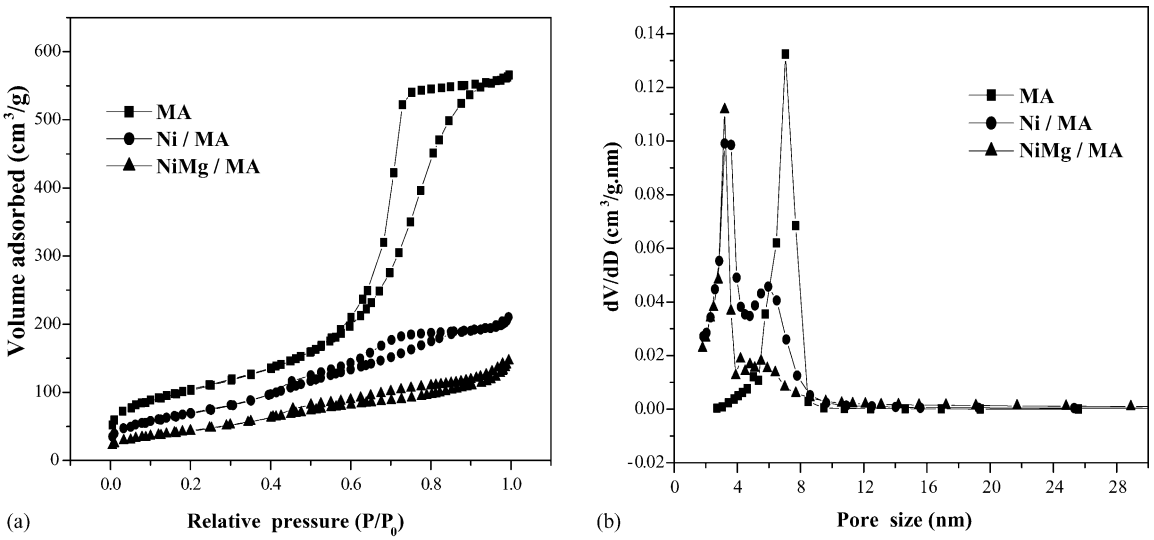

Fig. 2. (a) N_2 adsorption–desorption isotherms and (b) pore size distributions of mesoporous alumina (MA) and impregnated catalysts.

from ca. 0.5 to 0.8. It is known that the formation mechanism of chemical template containing metal source is strongly influenced by the solubility product value of the metal salt [11]. The K_{sp} value of metal chloride has an order of 10^1, while that of metal hydroxide has an order of 10^{-9}. This means that metal chloride is much more highly soluble in an aqueous solution than metal hydroxide. Therefore, it is inferred that metal chloride were mainly dissolved in the liquid phase and co-existed with stearate salt at low pH (HCl treatment), while metal hydroxide co-existed with stearate salt in the precipitate phase at high pH (NH_4OH treatment). This is the reason why NiMg-NP and NiMg-HS catalysts retained high metal contents with well-developed mesoporosity.

Fig. 2 shows the nitrogen isotherms and pore size distributions of bare alumina and impregnated catalysts. Compared to the bare alumina, the impregnated catalysts showed different isotherm patterns and pore size distributions. This indicates that aluminum dissolution and pore blocking by metal components occurred during the impregnation step, as previously reported [17,18]. Therefore, it is inferred from the results in Figs. 1 and 2 that the NiMg-NP and NiMg-HS catalysts may have advantages in catalytic applications over the conventional impregnated catalysts.

3.2. Phase transformation and particle size

XRD patterns of NiMg-HS and NiMg-NP catalysts are shown in Fig. 3. Although the presence of metal components was confirmed by ICP–AES measurements, no characteristic peaks indicating metal components were observed in the XRD patterns of the calcined catalysts. When metals such as Ni and Mg are supported on γ-Al_2O_3, metal particles are highly dispersed on the support via strong metal-support interaction, and sometimes, these metal particles are too small to be detected by XRD measurements [19,29]. On the other hand, the characteristic peaks for metallic Ni were observed in the XRD patterns of the reduced catalysts, indicating the formation of metal aggregation during the reduction step. Compared to the reduced NiMg-NP catalyst, the reduced NiMg-HS catalyst showed relatively sharp XRD peaks of metallic Ni species. This indicates that the NiMg-HS catalyst retained larger metal aggregation and lower metal dispersion than the NiMg-NP catalyst.

As shown in Fig. 4, it should be noted that the position of (4 4 0) diffraction peak of the impregnated catalysts shifted to the small diffraction angle compared to that of the bare alumina support (67.08°), indicating the metal incorporation into alumina lattice in the impregnated catalysts. The ionic radius

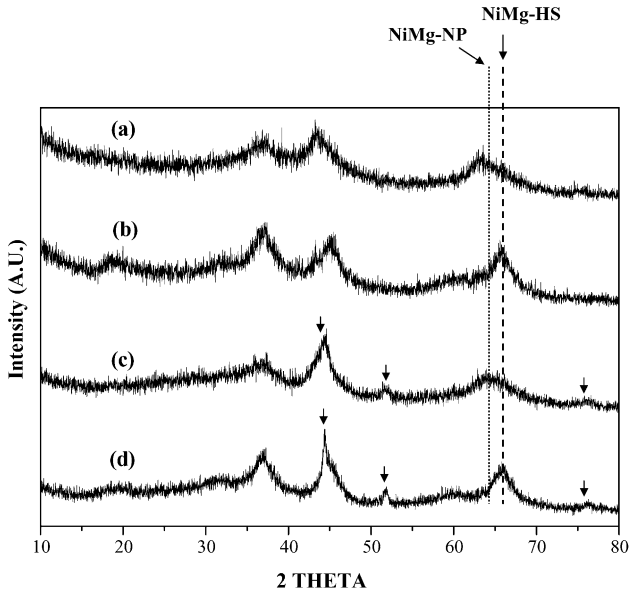

Fig. 3. XRD patterns of NiMg-Al_2O_3 catalysts: (a) calcined NiMg-NP, (b) calcined NiMg-HS, (c) reduced NiMg-NP, and (d) reduced NiMg-HS: vertical lines represent a (4 4 0) diffraction angle, (↓), Metallic Ni.

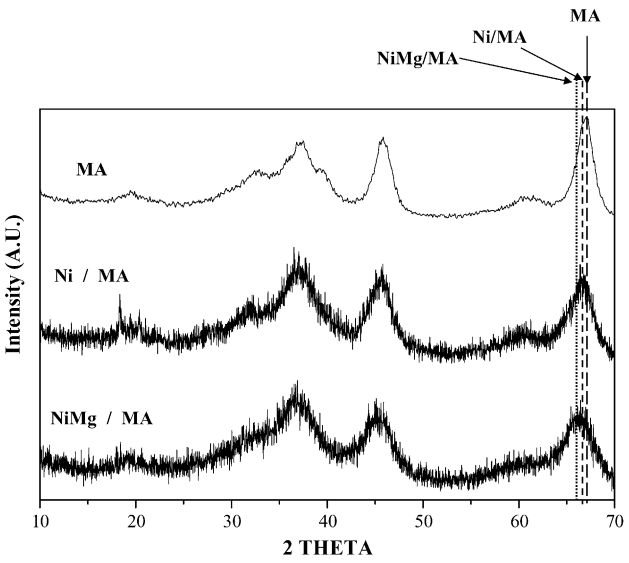

Fig. 4. XRD patterns of mesoporous alumina (MA) and impregnated catalysts after calcination: vertical lines represent a (4 4 0) diffraction angle.

of nickel or magnesium is larger than that of aluminum, and therefore, incorporation of metals leads to a lattice expansion of alumina, resulting in a shift of the diffraction peak [30,31]. Compared to the impregnated catalysts (66.64 and 66.28° for Ni/MA and NiMg/MA, respectively, Fig. 4), NiMg-Al_2O_3 catalysts experienced a large shift of (4 4 0) diffraction peak (64.90 and 65.53° for NiMg-NP and NiMg-HS, respectively, Fig. 3). These results suggest that the NiMg-Al_2O_3 catalysts are much more stable than the impregnated catalysts because metal incorporation leads to a decrease in the cationic deficiency of γ-Al_2O_3 [32].

TEM images of the reduced NiMg-Al_2O_3 catalysts are shown in Fig. 5. Some metal aggregations were observed in both catalysts, in good agreement with XRD results in Fig. 3. Additionally, the NiMg-NP and NiMg-HS catalysts retained their well-developed pore structure after the reduction at 450 °C.

3.3. Reducibility of NiMg-Al_2O_3 and impregnated catalysts

Fig. 6 shows the TPR patterns of NiMg-Al_2O_3 and impregnated catalysts. The TPR pattern of NiMg-HS catalyst is similar to that of NiMg/MA catalyst, where two reduction peaks were observed at below 450 and above 800 °C. On the other hand, the reduction peak of NiMg-NP catalyst appeared as a single broad one at around 600 °C. As shown in Fig. 6(b), the impregnated monometallic Ni/MA catalyst showed three reduction peaks at ca. 400, 630 and 800 °C. The TPR pattern of the supported metal catalyst generally reflects the physicochemical state of the metal component on the support, such as degree of metal-support interaction, oxidation state of the metal, and particle size of the metal species [33–38]. When nickel was impregnated on γ-Al_2O_3 and the catalyst was calcined under the mild conditions, the reduction peak at around 600 °C can be a typical characteristic peak of Ni/Al_2O_3 catalyst. The reduction peak at below 500 °C corresponds to easily reducible Ni species with a weak metal-support interaction, while the reduction peak at around 800 °C represents the nickel aluminate-like species. In the TPR pattern of the Ni/MA catalyst, therefore, the peaks at around 400 and 800 °C can be attributed to the reduction of nickel aggregates weakly interacted with alumina support and the reduction of nickel aluminate, respectively. It has been reported that nickel aluminate species were formed in the impregnated Ni/γ-Al_2O_3 catalysts after calcination at high temperature (usually above 600 °C) [39–41]. When considering the mild calcination conditions employed in this work, the formation of nickel aluminate species in the Ni/MA catalyst is quite unusual. However, this result may be attributed to the aluminum dissolution occurred during the impregnation step, as reported previously [17,18,42]. The formation of nickel aluminate in the NiMg/MA may be understood in a similar manner, as explained above for the Ni/MA catalyst. Therefore, it is reasonable to expect that the NiMg-HS catalyst prepared from an acidic solution experienced serious aluminum dissolution during the drying and calcination steps,

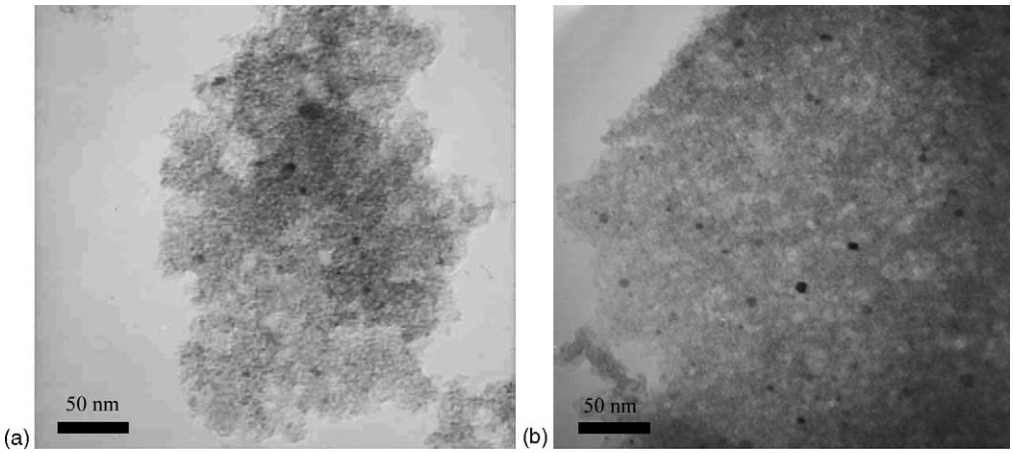

Fig. 5. TEM images of reduced NiMg-Al_2O_3 catalysts: (a) NiMg-NP and (b) NiMg-HS.

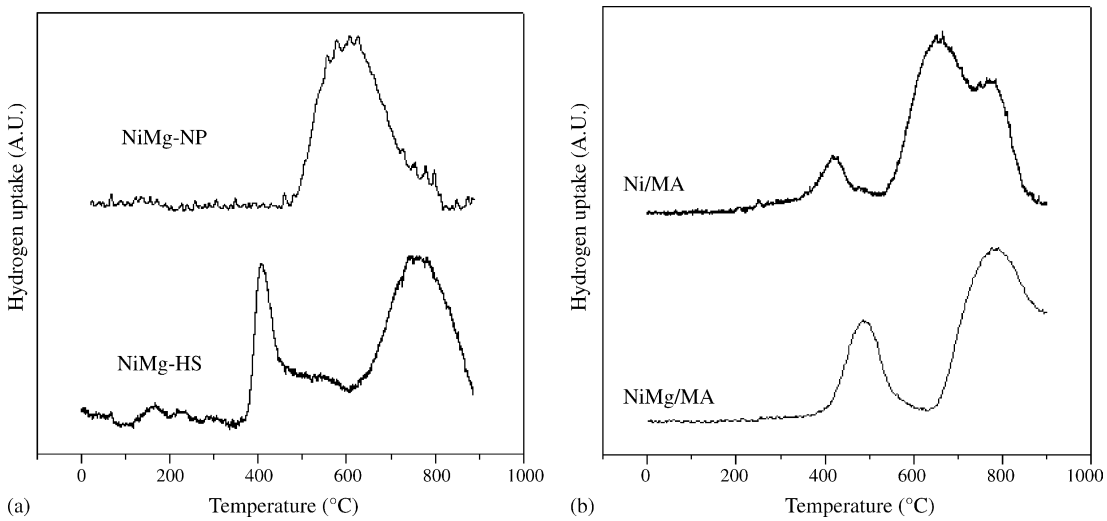

Fig. 6. TPR patterns of (a) NiMg-Al_2O_3 and (b) impregnated catalysts.

leading to the formation of nickel aluminate. Some metal aggregates of the impregnated catalysts, which are responsible for reduction peak appearing at around 400 °C, are likely to be formed during the mixing step, while those of the NiMg-HS catalyst are attributed to the solubility nature of metal chloride. As mentioned earlier, the solubility product value of metal chloride is very high, and therefore, metal chloride can serve as an additional metal source that does not interact with the template during the preparation of NiMg-HS. On the other hand, NiMg-NP catalyst shows a single broad reduction peak at around 600 °C. From this result, it is concluded that the NiMg-NP catalyst retained the highest level of homogeneity and dispersion of metal particles, among the catalysts employed in this work.

3.4. Hydrogen TPD profiles

In order to investigate, metal surface structure of the supported catalysts, hydrogen TPD measurements were carried out. Fig. 7 shows the hydrogen TPD profiles of supported catalysts. Although the TPD peak positions were slightly different from one another, the profiles could be divided into three regions; below 400 °C, around 600 °C, and above 800 °C. The TPD profiles at above 800 °C were not completely probed in this work. However, the occurrence of TPD peaks in this region is obvious judging from the trajectory of the signal. Undoubtedly, the TPD peak at above 800 °C can be ascribed to the reverse hydrogen spill-over [43], and the other two peaks can be assigned to different adsorption sites for hydrogen [44–46]. The NiMg-NP catalyst exhibited a stronger TPD signal at below 400 °C than the other catalysts, but the Ni/MA catalyst showed no TPD signal at this region. According to a literature [46], addition of Mg as a secondary metal can alter the electronic properties of Ni^0, leading to a weak interaction between hydrogen and metal phase, which can be confirmed by the appearance of intense TPD signal at low temperature region. It is expected that the electronic property of Ni^0 was changed more rigorously with increasing the mixing degree of Ni and Mg. This implies that Mg metals are more homogeneously mixed with Ni species in the NiMg-NP catalyst than those in the other catalysts. Therefore, it can be inferred that the metallic state in the NiMg-NP catalyst is more favorable for changing the electronic properties of the Ni^0.

3.5. Catalytic activity for hydrodechlorination of o-dichlorobenzene

Fig. 8 shows the typical catalytic activities of supported catalysts in the hydrodechlorination of *o*-dichlorobenzene. Compared to the monometallic Ni/MA catalyst, the bimetallic NiMg/MA exhibited the enhanced conversion and was considerably resistant against catalyst deactivation. Among the catalysts tested in this work, the MiMg-NP catalyst

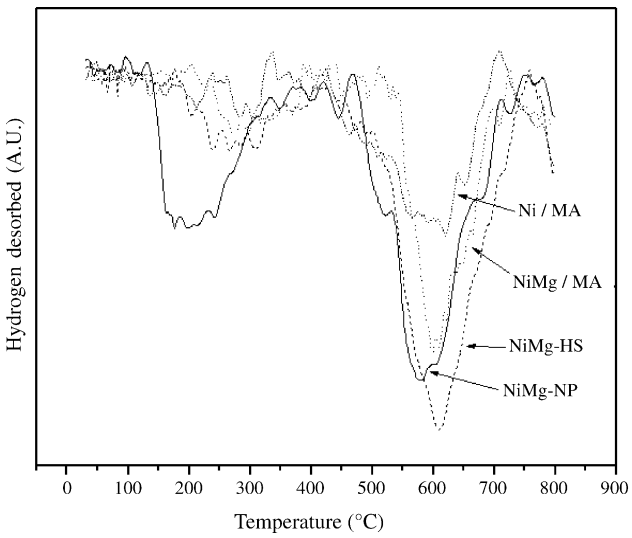

Fig. 7. Hydrogen TPD profiles of supported catalysts.

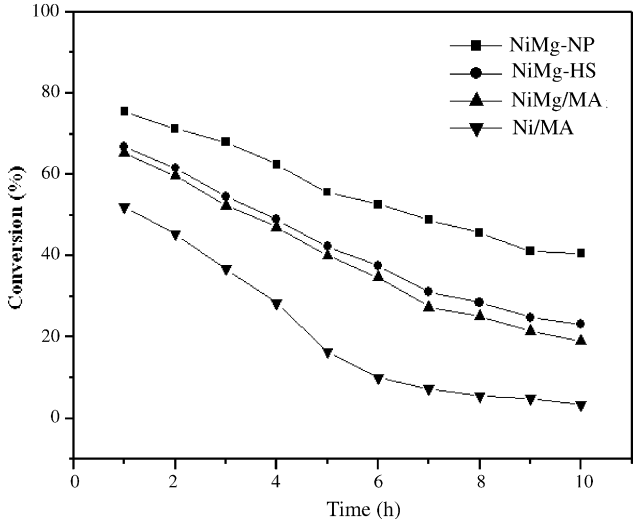

Fig. 8. Catalytic activities in the hydrodechlorination of *o*-dichlorobenzene.

showed the highest catalytic performance. This result is in good agreement with a previous observation in a sense that a catalyst showing a strong TPD signal at low temperature region might be highly active in the hydrodechlorination [46]. It is generally accepted that the catalyst deactivation observed in the hydrodechlorination reaction results from a poisoning by HCl produced during the reaction; HCl causes the transformation of active metallic nickel into $NiCl_2$ [25,26,46,47]. It is believed that the basic nature of magnesium oxide in the bimetallic catalyst preferably interacted with HCl, and thus, retarded catalyst deactivation [46]. The enhanced catalytic activity and suppressed catalyst deactivation of the NiMg-NP catalyst can also be attributed to the highly dispersed metallic nature of the catalyst. That is, magnesium oxides that are finely dispersed throughout the catalyst can serve as active sites for the reaction with HCl.

4. Conclusions

Bimetallic NiMg-Al_2O_3 catalysts were successfully prepared using chemical templates containing metal sources. The NiMg-NP and NiMg-HS catalysts exhibited well-developed framework mesoporosity and relatively high metal dispersion. Compared to the impregnated Ni/MA and NiMg/MA catalysts, the NiMg-NP and NiMg-HS catalysts showed more favorable pore structure for catalysis because pore blocking by metal components could be avoided. From the TPR measurements, it was observed that aluminum dissolution strongly affected the reducibility of Ni/MA, NiMg/MA, and NiMg-HS catalysts containing nickel aluminate species in their structures, while this effect was not observed in the NiMg-NP catalyst. The secondary metal, magnesium, played an important role in the formation of adsorption sites for hydrogen. The Ni/MA catalyst exhibited a very weak TPD signal at low temperature, while the bimetallic catalysts showed relatively strong peaks in the low temperature region. Because of the homogeneity of the mixed metallic state, NiMg-NP catalyst showed a stronger TPD signal at low temperature than NiMg-HS and NiMg/MA catalysts. The TPD results could be directly correlated with catalytic activities in the hydrodechlorination of *o*-dichlorobenzene. The NiMg-NP catalyst showing the most intense TPD peak at low temperature exhibited the highest catalytic activity in the reaction. The introduction of magnesium as a secondary metal was beneficial in retarding catalyst deactivation because magnesium oxides could readily react with HCl (a catalyst poison).

Acknowledgements

This work was supported by National Research Laboratory (NRL) program of the Korea Science and Engineering Foundation (KOSEF).

References

[1] C.T. Kresge, M.E. Leonowicz, W.J. Roth, J.C. Vartuli, J.S. Beck, Nature 359 (1992) 710.
[2] K.A. Koyano, T. Tatsumi, Microsc. Mater. 10 (1997) 259.
[3] Y. Kim, B. Lee, J. Yi, Korean J. Chem. Eng. 19 (2002) 908.
[4] A. Fuerte, M. Iglesias, F. Sanchez, A. Corma, J. Mol. Catal. A 211 (2004) 227.
[5] F. Vaudry, S. Khodabandeh, M.E. Davis, Chem. Mater. 8 (1996) 1451.
[6] S.B. Pu, J.B. Kim, M. Seno, T. Inui, Micro. Mater. 10 (1997) 25.
[7] Y. Liu, W. Zhang, T.J. Pinnavaia, Angew. Chem. Int. Ed. 40 (2001) 1255.
[8] Z. Zhang, Y. Han, L. Zhu, R. Wang, Y. Yu, S. Qiu, D. Zhao, F.-S. Xiao, Angew. Chem. Int. Ed. 40 (2001) 1258.
[9] S. Cabrera, J.E. Haskouri, J. Alamo, A. Beltran, S. Mendioroz, M.D. Marcos, P. Amoros, Adv. Mater. 11 (1999) 379.
[10] C. Kim, Y. Kim, P. Kim, J. Yi, Korean J. Chem. Eng. 20 (2003) 1142.
[11] Y. Kim, P. Kim, C. Kim, J. Yi, J. Mater. Chem. 13 (2003) 2353.
[12] Y. Kim, C. Kim, J.W. Choi, P. Kim, J. Yi, Stud. Surf. Sci. Catal. 146 (2003) 209.
[13] J.C. Park, J.H. Lee, P. Kim, J. Yi, Stud. Surf. Sci. Catal. 146 (2003) 109.
[14] Y. Park, T. Kang, Y.S. Cho, J.C. Park, P. Kim, J. Yi, Stud. Surf. Sci. Catal. 146 (2003) 637.
[15] M. Yada, M. Machida, T. Kijima, Chem. Commun. 6 (1996) 769.
[16] S.A. Bagshaw, T.J. Pinnavaia, Angew. Chem. Int. Ed. 35 (1996) 1102.
[17] P. Kim, Y. Kim, C. Kim, H. Kim, Y. Park, J.H. Lee, I.K. Song, J. Yi, Catal. Lett. 89 (2003) 185.
[18] P. Kim, Y. Kim, H. Kim, I.K. Song, J. Yi, J. Mol. Catal. A 219 (2004) 87.
[19] P. Kim, Y. Kim, H. Kim, I.K. Song, J. Yi, Appl. Catal. A 272 (2004) 157.
[20] N. Yao, G. Xiong, Y. Zhang, M. He, W. Yang, Catal. Today 68 (2001) 97.
[21] J. Cejka, Appl. Catal. A 254 (2003) 327.
[22] X. Zhang, F. Zhang, K.-Y. Chan, Mater. Lett. 58 (2004) 2782.
[23] T. Oikawa, T. Ookoshi, T. Tanaka, T. Yamamoto, M. Onaka, Mico. Meso. Mater. 74 (2004) 93.

[24] S.T. Srinivas, L.J. Lakshmi, N. Lingaiah, P.S.S. Prasad, P.K. Rao, Appl. Catal. A 135 (1996) 201.
[25] B. Coq, F. Figueras, J. Mol. Catal. A 173 (2001) 117.
[26] Y.H. Choi, W.Y. Lee, J. Mol. Catal. A 174 (2001) 193.
[27] P.P. Kulkarini, V.I. Kovalchuk, J.L. d'Itri, Appl. Catal. B 36 (2002) 299.
[28] D. Chakraborty, P.P. Kulkarni, V.I. Kovalchuk, J.L. d'Itri, Catal. Today 88 (2004) 169.
[29] F. Medina, P. Salagre, J.E. Sueiras, J.L.G. Fierro, J. Chem. Soc., Faraday Trans. 90 (1994) 1455.
[30] E.D. Dimotakis, T.J. Pinnavaia, Inorg. Chem. 29 (1990) 2393.
[31] A. Corma, V. Fornes, R.M. Martin-Aranda, F. Rey, J. Catal. 134 (1992) 58.
[32] J.A. Wang, A. Morales, X. Bokhimi, O. Novaro, Chem. Mater. 11 (1999) 308.
[33] J. Zielinski, J. Catal. 76 (1982) 157.
[34] G.R. Gavalas, C. Phichitkul, G.E. Voecks, J. Catal. 88 (1984) 54.
[35] P.K. De Bokx, W.B.A. Wassenberg, J.W. Geus, J. Catal. 104 (1987) 86.
[36] J.M. Rynkowski, T. Paryjczak, M. Lenik, Appl. Catal. A 106 (1992) 73.
[37] O. Dewaele, G.F. Froment, J. Catal. 184 (1999) 499.
[38] B.W. Hoffer, A.D. Langeveld, J.P. Janssens, R.L.C. Bonne, C.M. Lok, J.A. Moulijn, J. Catal. 192 (2000) 432.
[39] M.L. Jacono, M. Schiavello, A. Cimino, J. Phys. Chem. 75 (1971) 1044.
[40] M. Schiavello, M. Jacono, A. Cimino, J. Phys. Chem. 75 (1971) 1051.
[41] M. Houalla, B. Delmon, J. Phys. Chem. 84 (1980) 2194.
[42] J.A. Mieth, J.A. Schwarz, Appl. Catal. 55 (1989) 137.
[43] Z. Pa'al, P.G. Menon, Catal. Rev. Sci. Eng. 25 (1983) 229.
[44] Y. Cesteros, P. Salagre, F. Medina, J.E. Sueiras, Appl. Catal. B 22 (1999) 135.
[45] Y. Cesteros, P. Salagre, F. Medina, J.E. Sueiras, Appl. Catal. B 25 (2000) 213.
[46] Y. Cesteros, P. Salagre, F. Medina, J.E. Sueiras, D. Tichit, B. Coq, Appl. Catal. B 32 (2001) 25.
[47] B. Coq, G. Ferrat, F. Figueras, J. Catal. 101 (1986) 434.